BBA - Molecular Basis of Disease 1865 (2019) 1555–1566

Contents lists available at ScienceDirect

BBA - Molecular Basis of Disease

journal homepage: www.elsevier.com/locate/bbadis

Chemokine (C-C motif) ligand 2 gene ablation protects low-density lipoprotein and paraoxonase-1 double deficient mice from liver injury, oxidative stress and inflammation

Fedra Luciano-Mateo[a,b], Noemí Cabré[a,b], Salvador Fernández-Arroyo[a,b], Gerard Baiges-Gaya[b], Anna Hernández-Aguilera[a,b], Elisabet Rodríguez-Tomàs[b], Maria Mercado-Gómez[b], Javier A. Menendez[c,d], Jordi Camps[a,b,*], Jorge Joven[a,b,e,*]

[a] Universitat Rovira i Virgili, Department of Medicine and Surgery, Reus, Spain
[b] Unitat de Recerca Biomèdica, Hospital Universitari Sant Joan, Institut d'Investigació Sanitària Pere Virgili, Universitat Rovira i Virgili, Reus, Spain
[c] Program Against Cancer Therapeutic Resistance (ProCURE), Metabolism and Cancer Group, Catalan Institute of Oncology, Girona, Spain
[d] Girona Biomedical Research Institute (IDIBGI), Girona, Spain
[e] The Campus of International Excellence Southern Catalonia, Tarragona, Spain

ARTICLE INFO

Keywords:
Autophagy
Chemokine (C-C motif) ligand 2
Energy metabolism
Glutathione
Methionine cycle
Non-alcoholic fatty liver disease

ABSTRACT

The risk of non-alcoholic fatty liver disease increases with obesity. Vulnerability to oxidative stress and/or inflammation represents a crucial step in non-alcoholic fatty liver disease progression through abnormal metabolic responses. In this study, we investigated the role of CCL2 gene ablation in mice that were double deficient in low density lipoprotein receptor and in paraoxonase-1. Mass spectrometry methods were used to assess the liver metabolic response in mice fed either regular chow or a high-fat diet. Dietary fat caused liver steatosis, oxidative stress and the accumulation of pro-inflammatory macrophages in the livers of double deficient mice. We observed alterations in energy metabolism-related pathways and in metabolites associated with the methionine cycle and the glutathione reduction pathway. This metabolic response was associated with impaired autophagy. Conversely, when we established CCL2 deficiency, histologic features of fatty liver disease were abrogated, hepatic liver oxidative stress decreased, and anti-inflammatory macrophage marker expression levels increased. These changes were associated with the normalization of metabolic disturbances and increased lysosome-associated membrane protein 2, expression, which suggests enhanced chaperone-mediated autophagy. This study demonstrates that CCL2 is a key molecule for the development of metabolic and histological alterations in the liver of mice sensitive to the development of hyperlipidemia and hepatic steatosis, a finding with potential to identify new therapeutic targets in liver diseases.

Abbreviations: 4-HNE, 4-hydroxy-2-nonenal; AKT, protein kinase B; ALT, alanine aminotransferase; AMPK, AMP-activated protein kinase; AST, aspartate aminotransferase; Atg7, autophagy-related protein 7; CCL2, chemokine (C-C motif) ligand 2; CCR2, C-C chemokine receptor type 2; CD 11b, cluster of differentiation 11B; CD, standard diet; CD163, cluster of differentiation 163; CLEC4F, C-type lectin domain family 4 member F; CMA, chaperone mediated autophagy; CPLKO, triple deficient mice in CCL2, PON1 and LDLr; FAH, fumarylacetoacetate hydrolase; GC-MS-EI, gas chromatograph coupled to a quadrupole time-of-flight mass spectrometer with an electron impact source; GSH, glutathione; GSSG, glutathione disulfide; GTT, glucose tolerance test; HDL, high density lipoprotein; HFD, high fat diet; LAMP2A, lysosome associated membrane protein 2; LC3, microtubule-associated proteins 1A/1B light chain 3B; LDLr, low density lipoprotein receptor; mTOR, mammalian target of rapamycin; NADPH, nicotinamide adenine dinucleotide phosphate; NAFLD, non-alcoholic fatty liver disease; NASH, non-alcoholic steatohepatitis; P4EBP1, eukaryotic initiation factor 4E-binding protein 1; PI3K, phosphoinositide 3-kinase; PLKO, double deficient mice in PON1 and LDLr; PON1, paraoxonase-1; SAH, S –adenosylhomocysteine; SAM, S –adenosylmethionine; UHPLC, ultra-high-pressure liquid chromatography-quadrupole time of flight mass spectrometer

* Corresponding authors at: Unitat de Recerca Biomèdica, Hospital Universitari Sant Joan, Institut d'Investigació Sanitària Pere Virgili, Universitat Rovira i Virgili, Carrer Sant Joan s/n, 43201 Reus, Spain.
E-mail addresses: jcamps@grupsagessa.com (J. Camps), jjoven@grupsagessa.com (J. Joven).

https://doi.org/10.1016/j.bbadis.2019.03.006
Received 10 January 2019; Received in revised form 11 March 2019; Accepted 19 March 2019
Available online 21 March 2019

1. Introduction

The liver is vulnerable to inappropriate food ingestion, and ectopic fat accumulation induces non-alcoholic fatty liver disease (NAFLD). NAFLD has become the most common liver disease worldwide and encompasses a histological spectrum, ranging from simple steatosis to non-alcoholic steatohepatitis (NASH), which may progress to cirrhosis and hepatocellular carcinoma [1,2]. NASH is multifactorial and may be progressive, but the mechanisms affecting its development are too complex to be fully established in humans. Recent analytical tools are now available to explore the adaptive metabolic response to liver injury by examining the combined relationships among metabolic abnormalities, oxidative stress and inflammation, including paraoxonase 1 (PON1) and chemokine (C-C motif) ligand 2 (CCL2), as key molecules to understand the role of antioxidant defenses and monocyte recruitment in the liver [3–6]. PON1 may be found both in hepatocytes and in the circulation bound to lipoproteins and functions primarily as an effective molecule to modulate lipid peroxidation and the inflammatory response, likely influencing the production of CCL2 [7]. In this context, we have previously reported in experimental models that *pon1* deficiency or *ccl2* overexpression render mice prone to liver steatosis and metabolic alterations [8–10].

Excessive calorie intake is a major cause of liver injury and compromises the ability of hepatocytes to alter their metabolism (metabolic reprogramming) to trigger the adaptive response of intracellular sensors and signaling molecules necessary for liver homeostasis [11–13]. To be efficient, this adaptation requires substantial mitochondrial activity. However, oxidative stress and inflammation induce mitochondrial dysfunction and eventually cellular death, indicating that these processes and energy metabolism pathways may be interrelated and can interfere with reparative mechanisms [14]. Mechanistically, we hypothesize that the relationships among mitochondrial function and the roles of PON1 and CCL2 could be associated with at least two essential activities. The first involves the link between the citric acid cycle (CAC) and methionine and the consequent role in the maintenance of correct glutathione synthesis [15]. The second is associated with the regulation of autophagy-lysosomal function, an essential process for liver metabolic homeostasis that is highly dependent on AMP-activated protein kinase (AMPK)/mammalian target of rapamycin (mTOR) signaling in energy metabolism [16–18].

Herein, we explore the role of PON1 and CCL2 in liver disease and how oxidative stress and inflammation modulate hepatic intracellular signaling molecules and the adaptive metabolic response to fat-induced liver injury. Specifically, we investigated the alterations produced by the diet in mice triple deficient in the genes of low density lipoprotein receptor, PON1 and CCL2 (CPLKO mice), using as control groups wild type (WT) mice and mice double deficient in the low density lipoprotein receptor and PON1 (PLKO). These last animals have previously been used as a model of hyperlipidemia, hepatic steatosis and metabolic syndrome [8–10].

2. Results

2.1. Metabolic phenotypes, including liver histology and distribution of macrophages, were sensitive to CCL2 deficiency

PLKO and CPLKO mice had a significantly lower body weight than WT animals when given chow diet (CD). In contrast, weight increased similarly in all strains when fed high fat diet (HFD; Fig. 1A). Moreover, serum cholesterol, triglycerides and glucose concentrations were significantly higher in the HFD groups than in the CD groups, and PLKO and CPLKO mice had higher values than WT animals. All strains became glucose intolerant when fed HFD but without significant differences among strains, and serum glucose remained lower in mice with *ccl2* deficiency. Serum aspartate aminotransferase (AST) and alanine aminotransferase (ALT) activities were higher in PLKO mice than in WT animals, while CPLKO mice had levels of these enzymes similar to those of the WT group (Fig. 1B). These findings suggested a differential hepatic response that was confirmed histologically (Fig. 2). Minor fat accumulation was observed in PLKO mice fed CD, and prominent liver steatosis was observed when fed HFD. In contrast, CPLKO mice did not develop steatosis irrespective of the administered diet (Fig. 2A).

The immunohistochemical expression of 4-hydroxy-2-nonenal (4-HNE) was low in WT mice and very high in PLKO animals. The expression of 4-HNE in CPLKO mice was similar to that of WT animals, indicating a similar degree of oxidative stress (Fig. 2B). Again, the expected higher oxidative stress in *pon1*-deficient mice was averted by the added deficiency in *ccl2* (CPLKO), suggesting that CCL2 may potentially induce major metabolic changes, inhibit the inflammatory response, or both.

Differences between PLKO and CPLKO mice were observed through the differential abundance of liver macrophages with different phenotypes. PLKO mice fed a CD diet had a lower expression of C-type lectin domain family 4 member F (CLEC4F), indicating a lower amount of Kupffer cells. This alteration was corrected in CPLKO animals. However, we did not find any significant difference in this marker in mice given HFD (Fig. 3A). A significant subset of macrophages was positive for F4/80 antigen with expected potent phagocytic activity and reactive oxygen species (ROS) production capacity. PLKO mice did not change their relative abundance of these macrophages, but in mice deprived of *ccl2*, the relative proportion of F4/80+ cells remained significantly lower when fed either CD or HFD (Fig. 3B). A relatively low percentage of macrophages were positive for cluster of differentiation 11b (CD11b) staining, which increased in fat-challenged mice in all strains. CD11b is a marker of pro-inflammatory macrophages, and the increase was lower in CPLKO animals (Fig. 3C). Finally, to assess the putative reparative function of some macrophages and the functional adaptation to environmental challenges, we also measured CD163+ cells. This antigen is a marker of anti-inflammatory macrophages, and we found that PLKO mice had a significant decrease in the proportion of CD163-stained cells with respect to WT mice. The additional CCL2 deficiency counteracted such reduced expression (Fig. 3D). We also measured the hepatic mRNA expression of *CD11b* and *CD163*, which confirmed the immunohistochemical analyses in mice fed with CD, although we did not observe any significant differences in animals fed with HFD (Supplementary Fig. S1).

We used mice deficient in the C-C chemokine receptor type 2 (CCR2) gene to investigate whether CCR2-CCL2 signaling pathway is the responsible of the hepatic improvements observed in CPLKO mice. *Ccr2* deficient mice did not develop steatosis at 6 weeks of HFD treatment and showed a low amount of 4-HNE and F4/80 stained cells. These mice did not present any significant differences in the immunological stainings of CLEC4F, CD163 and CD11b with respect to WT animals (Supplementary Figs. S2 and S3).

Taken together, our findings indicate that CCL2 alters the metabolic phenotype of mice challenged with fat accumulation and may reshape the functional capacity of liver macrophages.

2.2. Oxidative stress and inflammation mediate energy metabolism-associated pathways

Targeted metabolomic analysis indicated that PLKO and CPLKO mice differ in their liver metabolism. Partial least square discriminant analysis visually indicates the role of the measured metabolites in discriminating among the different experimental groups. Separation among groups was more clearly shown in animals fed HFD, and the effects on the distribution among dietary groups were consistent. The standardized metabolite concentrations were represented as a heatmap, and most metabolites discriminated both genetic variations, including the effect of diet. Glycolysis and amino acid metabolism appear to be important to explain the differences superposed by *ccl2* deficiency, as shown by the ranked importance of metabolites without supervision via

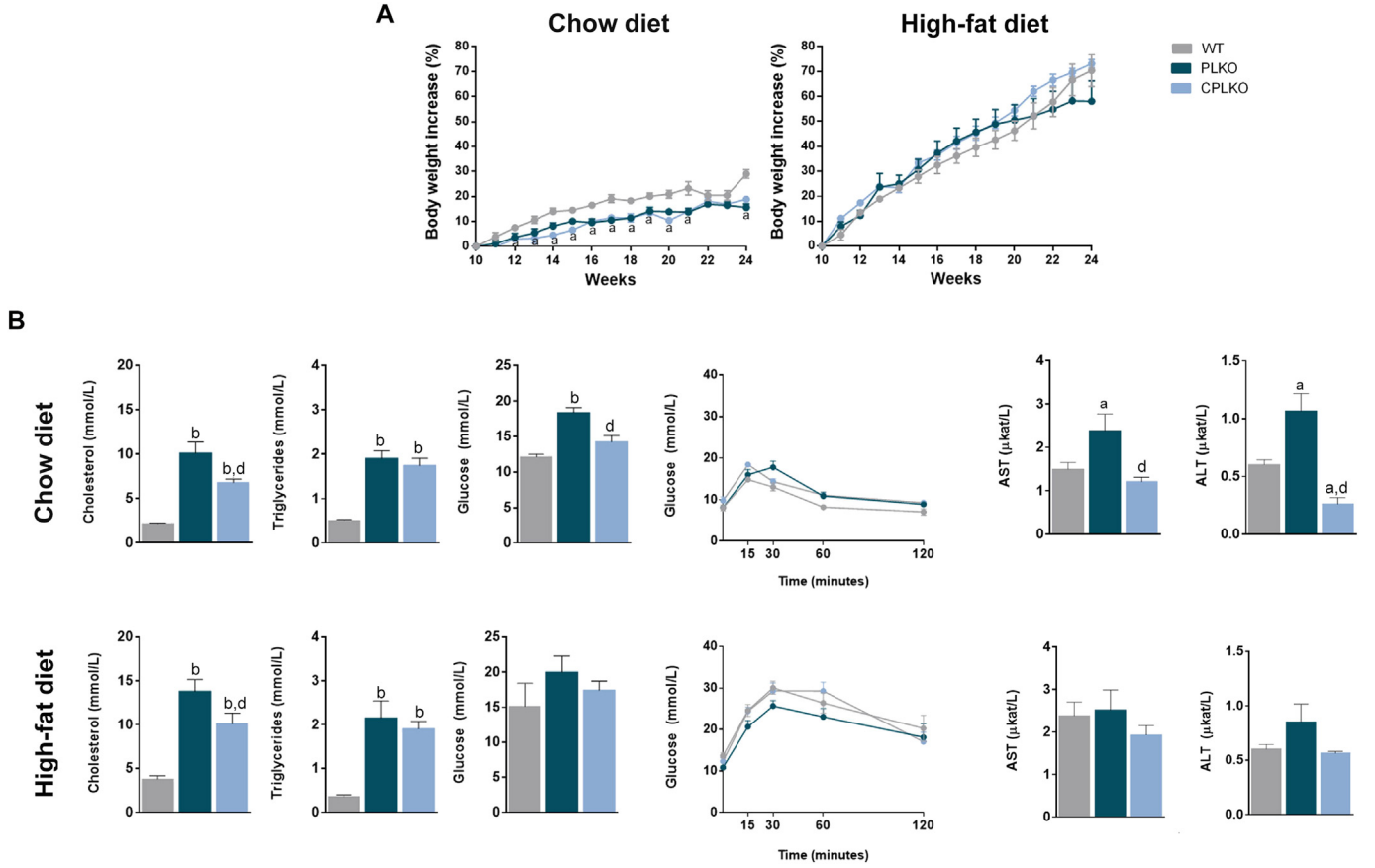

Fig. 1. Selected metabolic features in genetically modified mice. The results for (A) Body weight increase and (B) biochemical variables. PLKO denotes *ccl2*$^{+/+}$, *pon1*$^{-/-}$, *ldlr*$^{-/-}$ and CPLKO denotes *ccl2*$^{-/-}$, *pon1*$^{-/-}$, *ldlr*$^{-/-}$. Values are mean ± SEM (n = 8 per genotype and dietary condition) $^{a}P < 0.05$, $^{b}P < 0.001$, with respect to control littermates (WT); $^{c}P < 0.05$, $^{d}P < 0.001$, with respect to PLKO.

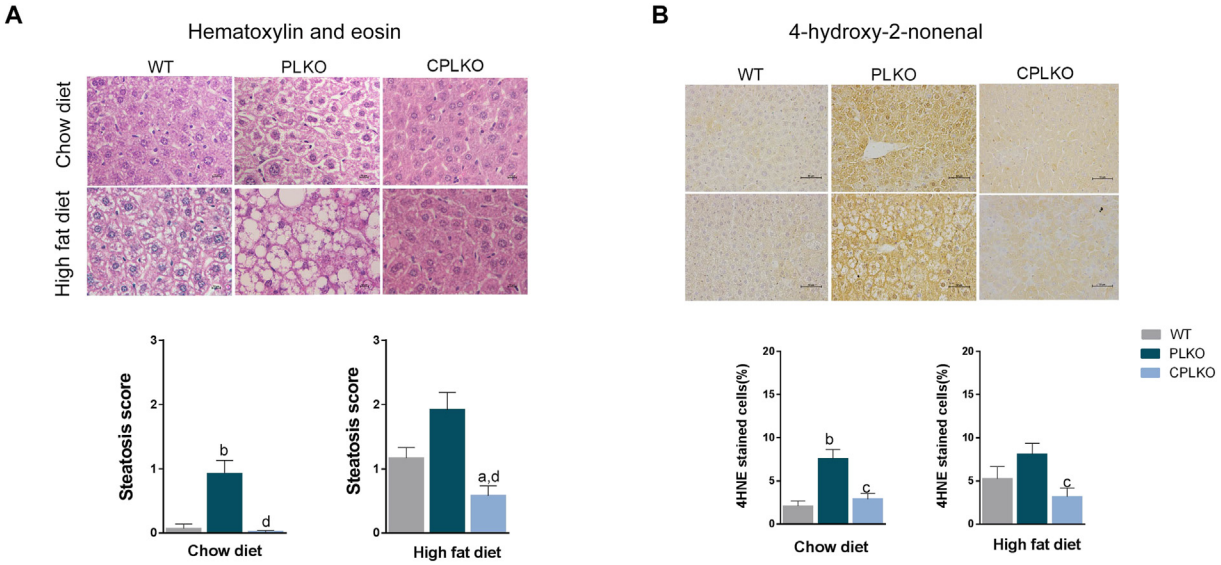

Fig. 2. Hepatic histological features. Representative microphotographs (bars indicate magnification) of liver sections stained with (A) hematoxylin and eosin and against (B) 4-hydroxy-2-nonenal (4-HNE). PLKO denotes *ccl2*$^{+/+}$, *pon1*$^{-/-}$, *ldlr*$^{-/-}$ and CPLKO denotes *ccl2*$^{-/-}$, *pon1*$^{-/-}$, *ldlr*$^{-/-}$. Values reported for the calculated steatosis score and 4HNE stained cells are mean ± SEM (n = 8 per genotype and dietary condition) $^{a}P < 0.05$, $^{b}P < 0.001$, with respect to control littermates (WT); $^{c}P < 0.05$, $^{d}P < 0.001$, with respect to PLKO.

random forest analysis (Fig. 4, Supplementary Table S1).

When comparing the metabolic response of PLKO and CPLKO mice with respect to normal (WT), we found an accumulation of glucose-6-phosphate together with increased proximal and distal metabolites, including fructose 6-phosphate, fructose 1,6-bisphosphate and ribose-5 phosphate, indicating a reduced entry of glucose carbon into mitochondrial biosynthetic metabolism and likely alterations in the pentose monophosphate shunt. In both strains, with minor dietary-induced

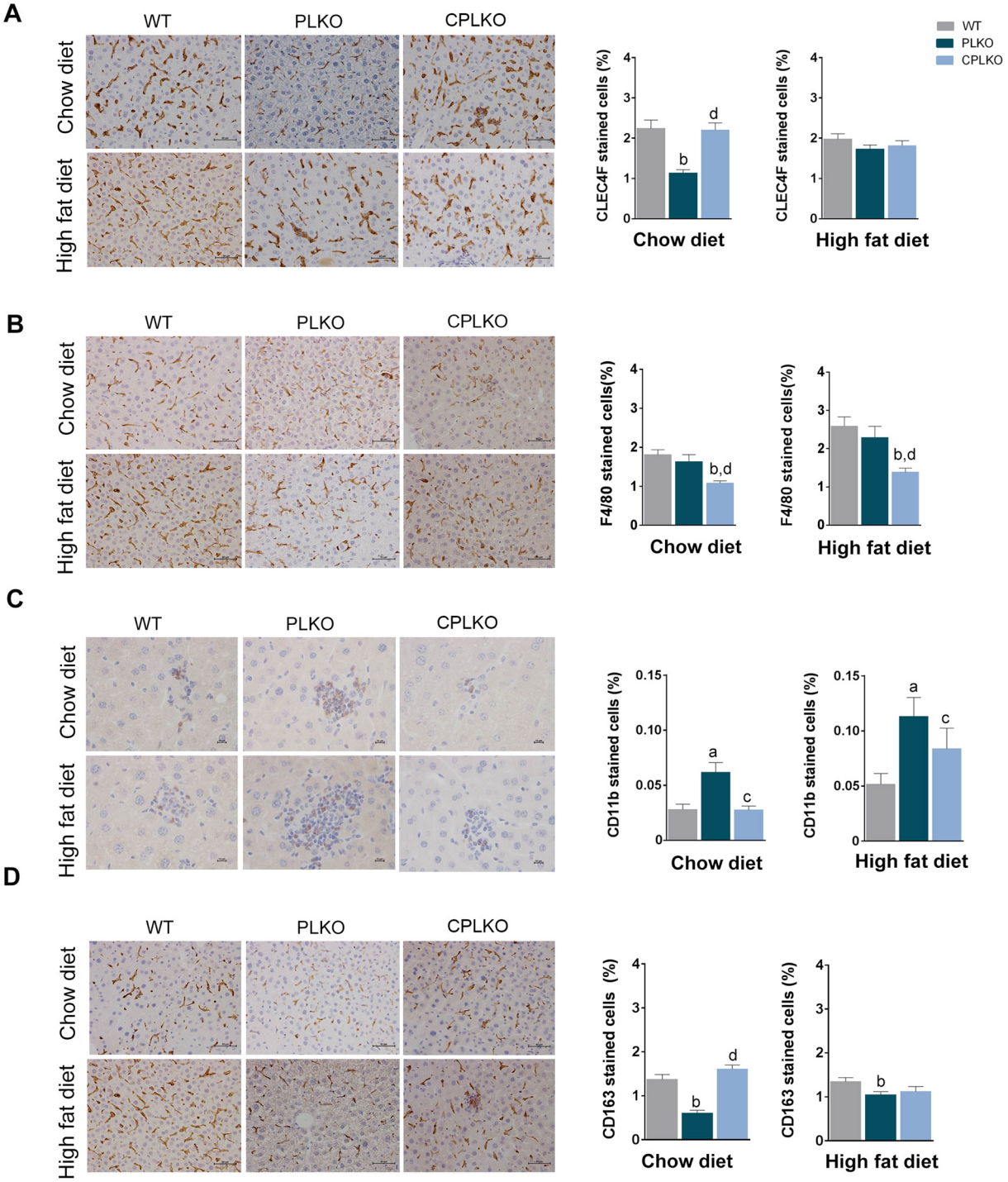

Fig. 3. Hepatic macrophage relative density. Representative microphotographs (bars indicate magnification) illustrating immunohistochemical staining of (A) C-type lectin domain family 4 member F (CLEC4F), (B) F4/80, (C) cluster of differentiation 11b (CD11b) and (D) cluster of differentiation 163 (CD163). PLKO denotes $ccl2^{+/+}$, $pon1^{-/-}$, $ldlr^{-/-}$ and CPLKO denotes $ccl2^{-/-}$, $pon1^{-/-}$, $ldlr^{-/-}$. Values for the calculated stained cells (%) are mean ± SEM (n = 8 per genotype and dietary condition) $^{a}P < 0.05$, $^{b}P < 0.001$, with respect to control littermates (WT); $^{c}P < 0.05$, $^{d}P < 0.001$, with respect to PLKO.

differences, there was an apparent decoupling between glycolysis and CAC (Fig. 5A, B). Therefore, the induced mutations result in a state of relatively reduced hepatic oxidative metabolism. However, the accumulation of lactate and β-hydroxybutyrate quantitatively differed according to the ingestion of calories and were more evident in comparisons between PLKO and CPLKO mice, suggesting potential alternatives to provide CAC feeding. Notably, mice deprived from CCL2 significantly improved the function of the glycolytic pathway and connections with CAC. Hepatic mitochondria also support relevant pathways related to the ability of 4-carbon intermediates to move into (anaplerosis) and out of (cataplerosis) the CAC without undergoing oxidation. These metabolic activities are required for shuttling reducing equivalents and biosynthetic substrates to other pathways, and the relative accumulation of CAC intermediates, lactate, ketone bodies and amino acids suggests that CCL2 may influence the flux of anaplerosis and cataplerosis-associated pathways (Fig. 5C). Taken together, our results suggest that PON1 and CCL2 are closely related and may affect metabolic activities with the potential for ROS formation in liver

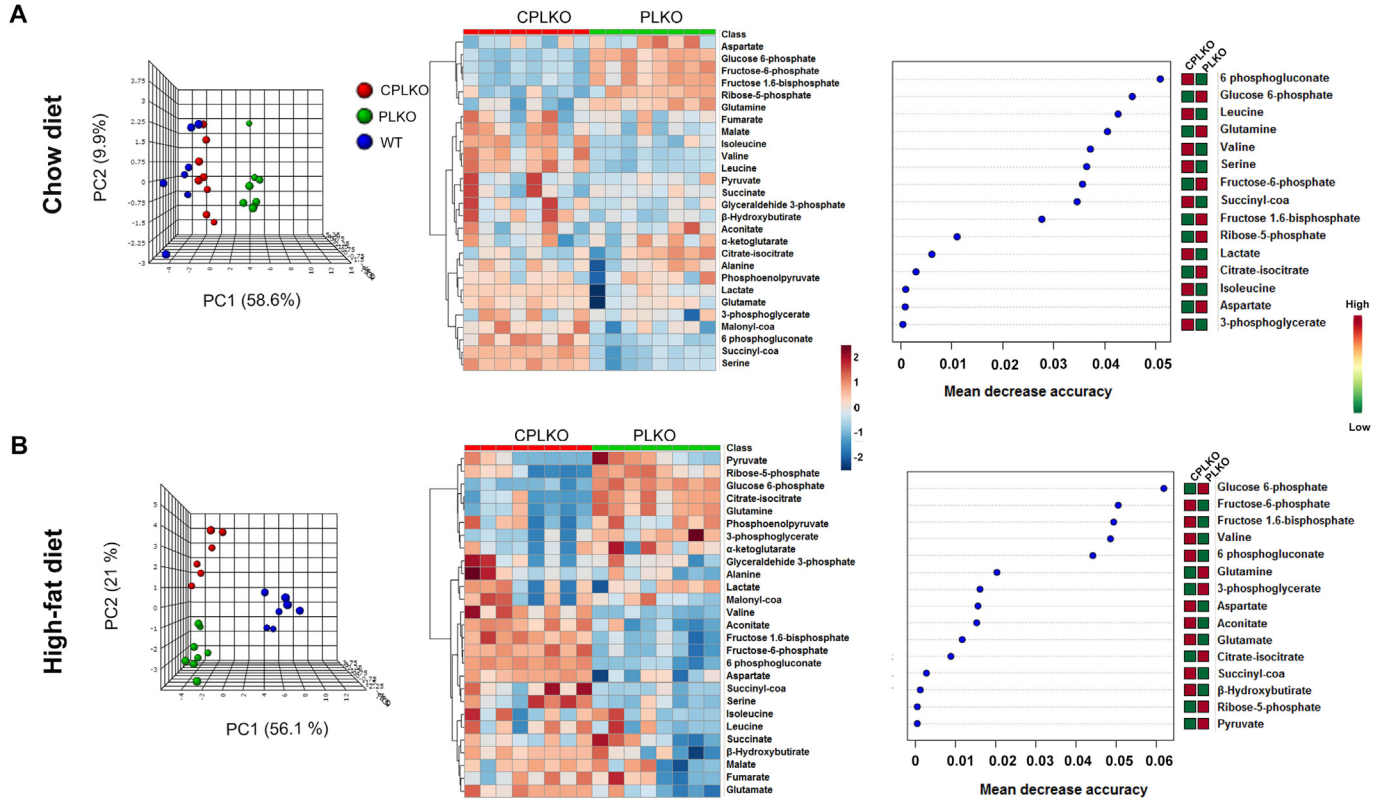

Fig. 4. Dietary-induced changes and the effect of *pon1* and/or *ccl2* ablation in hepatic energy-balance metabolites. From left to right in mice segregated by dietary conditions (A and B), partial least square discriminant analysis to visualize how measured metabolites discriminate among strains, heatmap built using standardized metabolite concentrations, and random forests to rank the importance of metabolites without supervision. PLKO denotes $ccl2^{+/+}$, $pon1^{-/-}$, $ldlr^{-/-}$ and CPLKO denotes $ccl2^{-/-}$, $pon1^{-/-}$, $ldlr^{-/-}$.

mitochondria, contributing to oxidative stress and inflammation under these conditions.

2.3. Oxidative stress-induced dysfunction in the liver methionine transmethylation and transsulfuration pathways may be restored by ccl2 deficiency

The liver regulates the flux of methionine through essential mechanisms affecting DNA, and protein methylation and the synthesis of the antioxidant glutathione. We observed significant differences in the levels of metabolites between PLKO and WT mice that were completely or partially averted in CPLKO animals (Supplementary Table S4, Fig. 6). For instance, there was a significant 4-fold decrease in methionine concentrations in PLKO mice when compared with the other strains, and the difference was maintained when fed CD or HFD. Homocysteine levels were also lower in PLKO mice, suggesting a significantly reduced flux in transmethylation. There were major changes in S-adenosylmethionine (SAM) and S-adenosylhomocysteine (SAH), substrate and product of essential methyltransferase reactions in PLKO mice. SAM levels were decreased in these animals, but differences only reached statistical significance when fed an HFD. In contrast, SAH levels increased dramatically, with a major impact on the SAM/SAH ratio. This decrease in the SAM/SAH ratio due to increased SAH correlated with homocysteine levels and probably suggests considerable alteration in the methylation status of hepatocytes. The SAM/SAH ratio in CPLKO mice was not different from that observed in WT mice, indicating reversal in causal mechanisms (Fig. 6). The reduced flux in methionine transmethylation of PLKO mice affects the efficient utilization of methionine for the synthesis of reduced glutathione (GSH) via the transsulfuration pathway. GSH is the most abundant antioxidant in hepatocytes and is critical for protecting cells from oxidative stress, acting as a free radical scavenger and inhibitor of lipid peroxidation. In PLKO mice, the GSH to GSSG ratio was extremely low, and we observed a greater mRNA expression of glutathione peroxidase and glutathione reductase than in WT and CPLKO animals (Supplementary Fig. S4). The GSH/GSSG ratio is an indicator of cellular health, and the reduced ratio indicates major cellular injuries because under normal conditions, reduced GSH represents up to 90% of cellular GSH. Interestingly, deficiency in CCL2 may be effective in maintaining hepatocytes' redox potential, but the levels were not completely reversed (Fig. 6). Our findings suggest that measurement of the GSH/GSSG ratio in the liver may bear usefulness in research focused on specific NAFLD therapeutics and the potential relationship between oxidative stress and epigenetic mechanisms.

2.4. Assessment of the role of ccl2 in hepatic autophagy-lysosomal function

In the liver, autophagy not only contributes to the maintenance of normal hepatocyte functions but also may respond to pathogenic changes. Autophagy was essentially suppressed or clearly reduced in genetically modified mice with respect to WT mice as assessed by low levels of microtubule-associated proteins 1A/1B light chain 3B (LC3) II/I ratio (Fig. 7), probably indicating a direct relationship with PON1 deficiency and high oxidative stress. We examined the autophagy-related protein 7 (Atg7), which was highly dependent on dietary conditions but did not significantly differ among strains. In contrast, mTOR was highly activated in genetically modified strains, as shown by the significant increase in the ratio between the phosphorylated and the nonphosphorylated forms. These changes probably refer to mTORC1 as indicated by a significantly higher expression of eukaryotic translation initiation factor 4E-binding protein 1 (P4EBP1) and were associated with low levels of AMPK activation. In addition, Akt was also highly

Fig. 5. The relative impact of dietary fat on the levels of metabolites associated with energy metabolism in the liver. Comparisons were made assessing fold-changes according to the legend in mice with *pon1* deficiency (A) and *pon1* and *ccl2* deficiency (B) with respect to control littermates and between both strains (C). PLKO denotes $ccl2^{+/+}$, $pon1^{-/-}$, $ldlr^{-/-}$ and CPLKO denotes $ccl2^{-/-}$, $pon1^{-/-}$, $ldlr^{-/-}$.

activated in PLKO and CPLKO mice. Considering the induced changes in liver histologic features and metabolic perturbations by the ablation of *ccl2* in PLKO mice, the lack of differential effects in the Akt/AMPK/mTOR pathway or the repression of autophagy appears noteworthy (Fig. 7). Then, we explored the expression of lysosome associated membrane protein 2 (LAMP2A), which was significantly increased in CPLKO mice with respect to PLKO mice levels, with even more dramatic effects when mice were fed HFD, suggesting a potential role of chaperone-mediated autophagy in the remission of oxidative stress (CMA). Taken together, our data indicate that PON1 deficiency is associated with decreased autophagosome formation, which is independent of CCL2. In contrast, CCL2 might affect CMA.

3. Discussion

In PLKO mice we found important liver alterations and energy stress. However, the additional ablation of CCL2, a key chemokine involved in the inflammatory response, partially or completely reverted most alterations in biochemical and histologic features. Essentially, we demonstrate the entwined roles of PON1 and CCL2 on the adaptive metabolic response to liver injury. Unbalanced nutritional status may lead to the accumulation of fat in hepatocytes, which sequentially induces mitochondrial dysfunction, oxidative stress, inflammation, and cell death. Remission through dietary interventions is uncommon, and our findings might have therapeutic and pathogenic implications in searching effective treatment procedures to reverse NAFLD and/or avoiding progression from simple steatosis to NASH.

The mechanisms establishing metabolic reprogramming in hepatocytes remains poorly understood. Overnutrition is causal in the altered expression of genes relevant for metabolism, oxidative stress and inflammation inducing epigenetic mechanisms responsible for the remarkable capacity of hepatocytes to switch their phenotypic status [9,19–21]. Hence, prevention of obesity and dietary restraint is a crucial first step in protecting the liver [22]. Reversibility of epigenetic mechanisms provides an interface between the host and environment. Here, we provide evidence indicating that oxidative stress probably interferes in the course of DNA and protein methylation through methionine metabolism and glutathione oxidation. The course of action may be substantially reversed, avoiding inflammation, which may provide a converging point between PON1 and CCL2 and are key mechanisms to explain the usefulness of epigenetic intervention through nutrition and drugs such as metformin and aspirin [23].

Our analysis of the coupled oxidation-inflammation system reveals in vivo a pivotal role in liver disease and potential alternative strategies capable of delaying NAFLD development. Deprivation of PON1, an important component of antioxidant defenses, results in increased

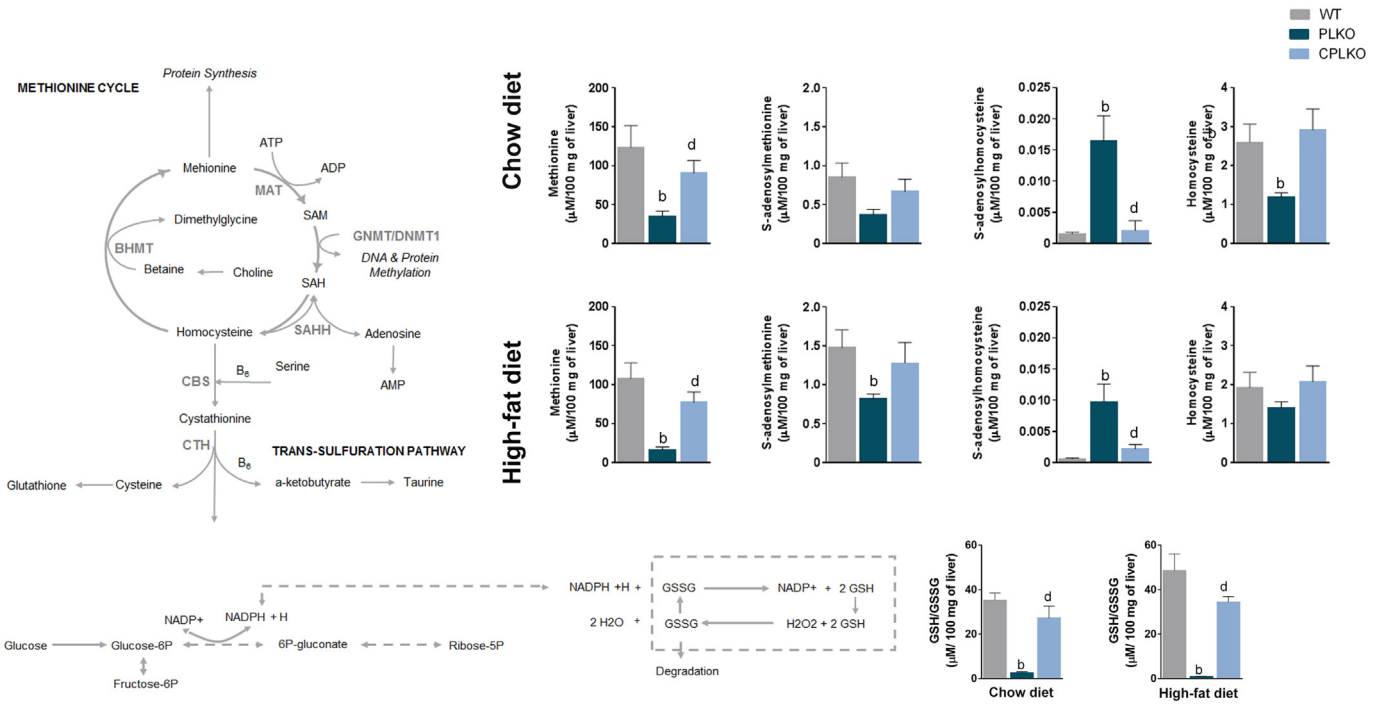

Fig. 6. The relative impact of dietary fat on the levels of metabolites associated with the methionine cycle and transsulfuration pathways in the liver. PLKO denotes *ccl2*$^{+/+}$, *pon1*$^{-/-}$, *ldlr*$^{-/-}$ and CPLKO denotes *ccl2*$^{-/-}$, *pon1*$^{-/-}$, *ldlr*$^{-/-}$. Values are mean ± SEM (n = 8 per genotype and dietary condition) $^{b}P < 0.001$, with respect to WT; $^{d}P < 0.001$, with respect to PLKO.

production of lipid peroxides, which correlated with fat accumulation and variations in the distribution of liver macrophages. Examination of energy metabolism in the livers of *pon1*-deficient mice suggested mitochondrial damage and decoupling from glycolysis, confirming that mitochondrial metabolism mediates oxidative stress and inflammation in fatty liver [24]. Mitochondrial damage can cause an imbalance between ROS production and removal, resulting in net ROS production. Potentially, overexpression of antioxidant defenses might improve lifespan and healthspan in mice [25]. The increase in glutathione peroxidase and glutathione reductase expression in PLKO mice can be interpreted as a mechanism of hepatocytes to defend against oxidative stress. Consequently, the GSH/GSSG ratio in these mice was extremely low in PLKO mice. This effect was also accompanied by a relative deficiency in methyl donors resembling the pro-oxidant, pro-inflammatory disturbances observed in mice fed methionine-choline deficient mice. Interestingly, most defects were completely reversed by the concomitant *ccl2* deficiency, most likely mediated by amelioration in macrophage functionality [26,27]. Although the liver has several types of immune cells such as natural killer cells, natural killer T cells, neutrophils, γδT cells, dendritic cells and lymphocytes T and B, macrophages represent one third of hepatic non-parenchymal cells and are considered the first response to liver injury, playing a major role in repair and regeneration processes [28].

Energy metabolism in the livers of CPLKO mice was also partially restored when compared with PLKO mice and suggested an important role of lactate and β-hydroxybutyrate as primary CAC substrates and in controlling the release of pro-inflammatory cytokines [29,30]. In addition, the restoration of branched chain amino acid metabolism observed in CPLKO mice might also contribute to the alleviation of liver steatosis and liver injury [31].

The AMPK signaling pathway coordinates autophagy and metabolism [32]. The heterotrimeric (αβγ) complex AMPK is a key player in maintaining cellular energy balance, and in these genetically modified mice, activation through phosphorylation at T172 of its catalytic subunit is significantly inhibited. Oxidative stress and energy stress may also differentially regulate AMPK activity through oxidation at several cysteine residues, a mechanism apparently dependent on the source of ROS, abundance of nutrients and the antioxidant capacity of cells [33]. AMPK activity and mTORC1 activation were inversely related, and autophagy was inhibited in both PLKO and CPLKO mice precluding the conjugation of LC3-I to phosphatidylethanolamine (LC3-II), which induced a low LC3-II/LC3-I ratio [34]. Therefore, the livers of these mice were deprived of a crucial mechanism to cope with a variety of cellular stresses. However, when we examined LAMP2A as a proxy for chaperone-mediated autophagy (CMA), we found that *pon1* deficiency altered this mechanism, which was completely reversed by the addition of *ccl2* deficiency. Accumulating evidence highlights the importance of autophagy in the maintenance of liver homeostasis and the involvement in the pathogenesis of NAFLD affecting hepatocytes and other hepatic cell types [18,35,36]. Our results suggest a possible link between CMA and NAFLD progression. CMA participates in protein quality control by degrading oxidized and damaged proteins under stress conditions and contributes amino acids through the degradation of proteins. The role of CMA in cellular fate has already been established by modulating carbohydrate and lipid metabolism, transcriptional programs, immune responses and the cell cycle through selective degradation of key enzymes in these pathways [37–39]. Indeed, it has been reported that high lipid concentrations can stimulate LAMP2A degradation through the modification of the lysosome membranes [40].

Previous studies suggest that the heterogeneous histological grades found in human biopsies were proportional to oxidative flux [24]. Our findings suggest that PON1 and CCL2 are key molecules modulating hepatic oxidative stress and inflammation that appear to be associated with increased oxidative metabolism, likely altering anabolic pathways. Both molecules are circulating in the blood at easily measurable concentrations and may represent possible predictive and diagnostic biomarkers of liver disease, but future research requires standardization of reagents and methods to overcome difficulties in interpretation [7]. Data may also suggest and/or potentiate novel therapeutic targets, which is important because there is no specific pharmacotherapy approved for NAFLD. For instance, it is plausible that increased PON1 activity may have beneficial effects in humans. Molecular mechanisms

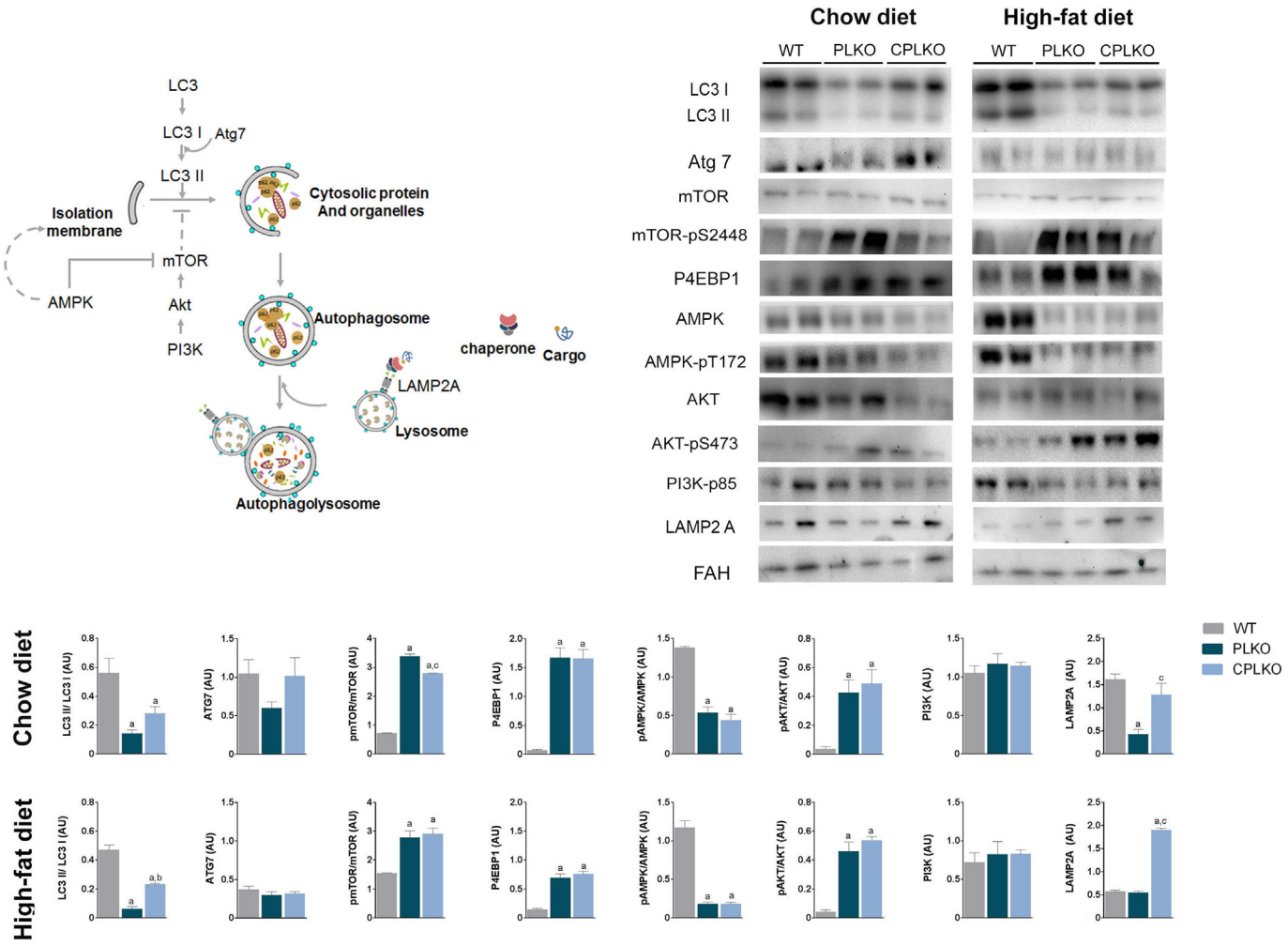

Fig. 7. Overall assessment of autophagy-lysosomal function through Western blot analysis of selected molecules, including microtubule-associated protein 1A/1B light chain 3B (LC3), autophagy-related protein 7 (Atg7), mammalian target of rapamycin (mTOR), mTOR-p S448, eukaryotic translation initiation factor 4E-binding protein 1 (P4EBP1), AMP-activated protein kinase (AMPK) AMPK-p T172, protein kinase B (AKT), AKT-pS473, phosphoinositide 3-kinase p85 subunit (PI3K-p85), lysosome associated membrane protein 2 (LAMP2A), and fumarylacetoacetate hydrolase (FAH). PLKO denotes *ccl2*$^{+/+}$, *pon1*$^{-/-}$, *ldlr*$^{-/-}$ and CPLKO denotes *ccl2*$^{-/-}$, *pon1*$^{-/-}$, *ldlr*$^{-/-}$. Representative bands are from pooled liver homogenates from randomly selected samples. Values for calculations are mean ± SEM (n = 8 per genotype and dietary condition); $^{a}P < 0.05$, $^{b}P < 0.01$, with respect to WT; $^{c}P < 0.05$, with respect to PLKO.

involved in the regulation of hepatic PON1 gene expression have not been explored, but several compounds may increase gene transcription, including probucol, several statins, vitamins and polyphenols (e.g., quercetin, naringenin, catechins, punicalagins, silymarin, and resveratrol) [41]. Similarly, polyphenol-rich foods may modulate plasma CCL2 in humans [42], and several anti-CCL2 antibodies and antagonists of its functional receptor (CCR2) are currently under investigation. Preclinical and clinical data on the dual CCR2/CCR5 inhibitor cenicriviroc are advanced in the path to approval (phase 3 trial) to specifically manage NASH and liver fibrosis [43,44]. Finally, our data also suggest that combination therapies are more likely to benefit patients with NAFLD than a single therapy and that drugs that may target AMPK activity and/or autophagy might be useful.

In summary, this study demonstrates that CCL2 is a key molecule for the development of metabolic and histological alterations in the liver of mice sensitive to the development of hyperlipidemia and hepatic steatosis, a finding with potential to identify new therapeutic targets in liver diseases.

4. Materials and methods

4.1. Mice generation, genotyping and experimental design

Low density lipoprotein receptor single deficient mice (*Ldlr*$^{-/-}$) and CCL2 single deficient mice (*ccl2*$^{-/-}$) were purchased from Jackson Laboratories (Bar Harbor, Maine, USA) and the University of California in Los Angeles kindly donated *pon1*$^{-/-}$ mice. All strains were backcrossed > 10 generations to ensure C57BL/6J genetic background. From their progeny, we first generated by breeding double-deficient mice in *pon1* and *ldlr* (*pon1*$^{-/-}$, *ldlr*$^{-/-}$; PLKO). Then, we generated another strain adding *ccl2* deficiency (*ccl2*$^{-/-}$, *pon1*$^{-/-}$, *ldlr*$^{-/-}$; CPLKO). PLKO mice and littermates without mutations (wild type, WT) were used as controls to investigate the effects of CCL2 deficiency. For some additional experiments, we used CCR2 single deficient mice (*Ccr*$^{-/-}$) purchased from Jackson Laboratories (Bar Harbor, Maine, USA), and fed a HFD.

Mice genotyping was performed using DNA isolated from the tail. *ccl2* and/or *pon1* mRNA expressions were analyzed from homogenized tails (Fig. 8) and livers (Supplementary Fig. S5) [45,46]. Handling of animals was performed by dedicated staff in accordance with current regulations and supervision by the Ethics Committee on Animal

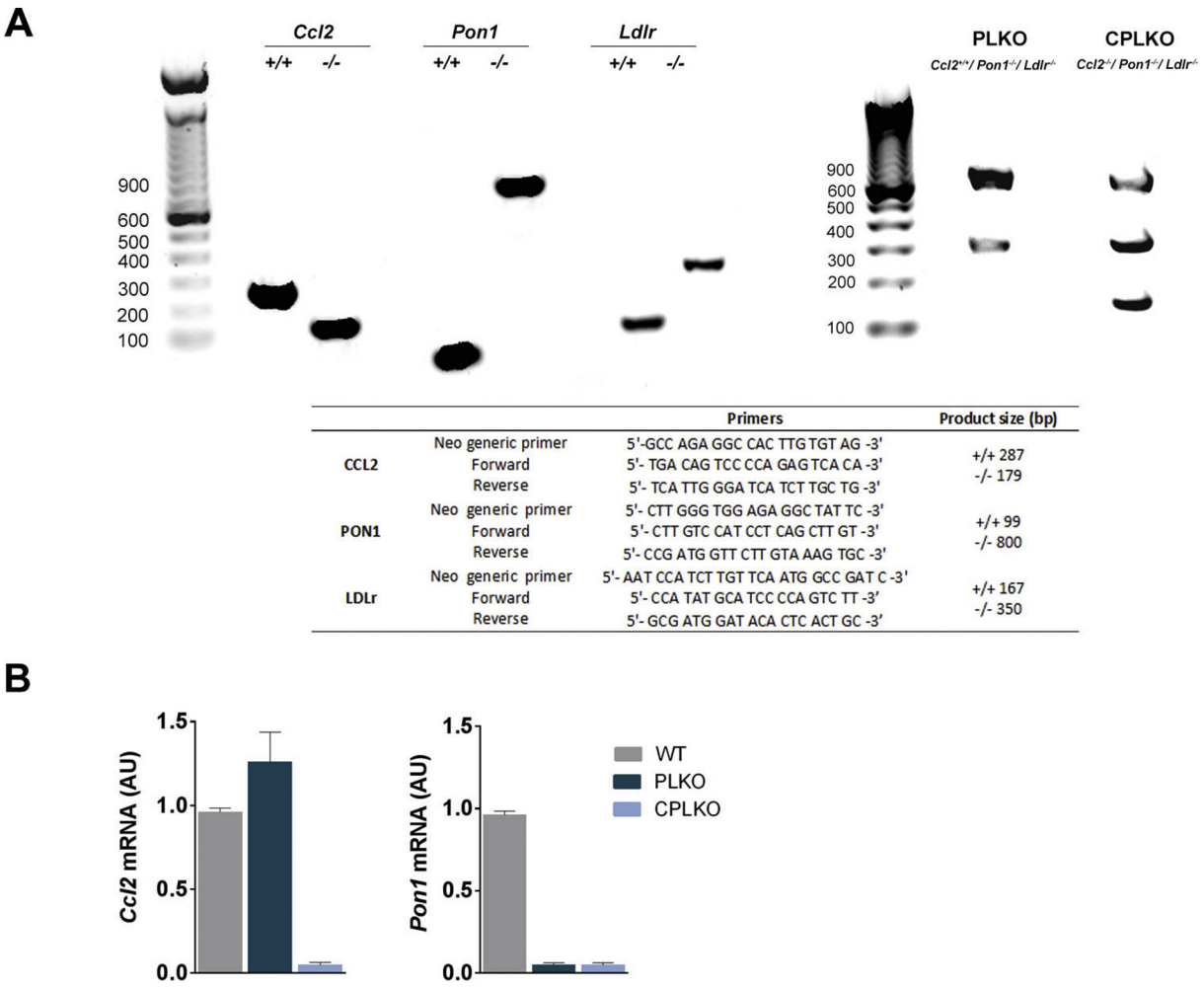

		Primers	Product size (bp)
CCL2	Neo generic primer	5'-GCC AGA GGC CAC TTG TGT AG -3'	+/+ 287 -/- 179
	Forward	5'- TGA CAG TCC CCA GAG TCA CA -3'	
	Reverse	5'- TCA TTG GGA TCA TCT TGC TG -3'	
PON1	Neo generic primer	5'- CTT GGG TGG AGA GGC TAT TC -3'	+/+ 99 -/- 800
	Forward	5'- CTT GTC CAT CCT CAG CTT GT -3'	
	Reverse	5'- CCG ATG GTT CTT GTA AAG TGC -3'	
LDLr	Neo generic primer	5'- AAT CCA TCT TGT TCA ATG GCC GAT C -3'	+/+ 167 -/- 350
	Forward	5'- CCA TAT GCA TCC CCA GTC TT -3'	
	Reverse	5'- GCG ATG GAT ACA CTC ACT GC -3'	

Fig. 8. Genotyping and liver mRNA expression in mice generation. (A) Electrophoretic assessment and primers used in genotyping. (B) Expression of *pon1* and *ccl2* mRNA in liver homogenates of 24-week-old male genetically modified mice and control littermates (WT). PLKO denotes $ccl2^{+/+}$, $pon1^{-/-}$, $ldl^{-/-}$ and CPLKO denotes $ccl2^{-/-}$, $pon1^{-/-}$, $ldlr^{-/-}$.

Experimentation of the Universitat Rovira i Virgili (protocols 4815 and GC-URV-0235-03.18.2014) following European guidelines (Directive 2010/63/EU).

Homozygous strains were viable and reproduced without difficulty under controlled temperature (22 °C), humidity (50%) and light/dark cycle 12/12 h in a stress-free environment and fed a CD prepared by Scientific Animal Food & Engineering, Augy, France and water ad libitum. The animals were randomly allocated to experimental groups, and the investigators responsible for the assessment of outcomes had no previous knowledge of the experimental group to which the animals belonged. No animals were excluded from the analysis. Selected male CPLKO, PLKO and WT mice (n = 16, each) at 10 weeks of age were allocated into two dietary groups (n = 8, each) to compare the *pon1*- and *ccl2*-related effects and to assess the differential response against caloric intake provided by CD or HFD (Ssniff Spezialdiäten GmbH, Soest, Germany), over 14 weeks. At the beginning of the study, other littermates (n = 3–4 for each strain) were used to confirm similar histologic features in their livers at this age. Information on supplied nutrients by both diets may be found in Supplementary Table S1.

4.2. Sample collection and biochemical analyses

One week before sacrifice, glucose tolerance tests (GTT) were performed on fasted (4 h) mice after intraperitoneal glucose (2 g/kg body weight) administration. Glucose concentrations were determined in blood from the tail immediately before and 15, 30, 60 and 120 min with test strips adapted to the Accuchek sensor system (Roche Diagnostics, Barcelona, Spain). At sacrifice, blood was obtained by intracardiac puncture to measure serum glucose, cholesterol, and triglyceride concentrations, and AST and ALT activities in an automated analyzer Roche Cobas Mira Plus (Roche Diagnostics).

4.3. Quantitative RT-PCR

Total RNA was extracted using the RNeasy kit (Qiagen, Barcelona, Spain) and was retrotranscribed using the Reverse Transcription System kit (Applied Biosystems; Invitrogen, Barcelona, Spain). Real-time PCR (qPCR) was conducted on a 7900HT Fast Real-Time PCR System using TaqMan Gene Expression Assays (Applied Biosystems). The results normalized according to the expression level of Beta-2-Microglobulin (B2M) mRNA.

4.4. Histological analyses and immunochemistry

Livers were frozen in liquid N_2 and stored at −80 °C and/or fixed in formalin (formaldehyde 3.7–4% buffered to pH = 7 and stabilized with methanol 1–1.5%) until analysis. Adequate sections were stained with hematoxylin and eosin to evaluate liver impairment according to a scoring system as described [47]. For immunohistochemistry, procedures were performed as described with few modifications [46]. Briefly,

after deparaffinization and rehydration of 2 μm liver sections, antigens were retrieved in 0.15 mol/L sodium citrate or Tris 10 mM/EDTA 1 mM buffer at pH = 6 or pH = 9 in a microwave oven until reaching 90 °C. Bovine serum albumin (2%) and hydrogen peroxide (1%) were sequentially used to block nonspecific binding sites and endogenous peroxidase and rinsed with phosphate buffered saline. Then, sections were incubated with the corresponding primary antibody, the appropriate secondary antibody and detected with reagents described in Supplementary Table S2. All sections were counterstained with Mayer's hematoxylin and quantified via image analysis (at least 10 fields for each sample) using ImageJ software (National Institutes of Health, USA). To assess differences in oxidation and inflammation and to explore macrophage heterogeneity in healthy and diseased liver, we stained macrophages for CLEC4F, antigen F4/80, CD11b, CD163, and 4-HNE [11,48,49].

4.5. Western blot analyses

Frozen liver tissue (20 mg) from each animal was homogenized in 300 μL of lysis buffer composed of 0.25 M sucrose, 1 mM Pefabloc SC (Sigma-Aldrich, Saint Louis, MI, USA), and a phosphatase inhibitor cocktail (Hoffman-La Roche, Basel, Switzerland) using a sonicator (Branson Sonifer 150, Thistle Scientific, Glasgow, UK). Western blotting was performed by denaturing 50 μg of protein at 100 °C for 5 min in Laemmli sample buffer and β-mercaptoethanol. For protein separation, 8%–14% sodium dodecyl sulfate-polyacrylamide gel was used, and proteins were transferred onto a polyvinylidene difluoride or nitrocellulose membrane (Thermo Fisher, Barcelona, Spain). Before the primary antibody incubation, membranes were blocked with nonfat milk or bovine serum albumin at 5% in Tris, sodium chloride and 1% Tween-20 (pH = 7.4). Reagents and further details may be found in Supplementary Table S2. Bands were detected with a SuperSignal West Femto chemiluminescent substrate (Pierce, Rockford, IL, USA), and the analysis was performed with a ChemiDoc system (Bio-Rad Laboratories, Madrid, Spain). Bands were analyzed and quantified using Image Lab 2.0 software (Bio-Rad Laboratories). Specifically, we measured the expression of molecules involved in the regulation of energy metabolism and autophagy-lysosomal function, including the phosphoinositide 3-kinase p85 subunit (PI3K-p85), protein kinase B (AKT), phospho-AKT Ser 473 (AKT- pS473), mTOR, phospho-mTOR Ser 2448 (mTOR-pS2448), AMPK, AMPK- pT172, eukaryotic translation initiation factor 4E-binding protein 1 (P4EBP1), the microtubule-associated protein 1A/1B light chain 3B (LC3-I and LC3-II) and LAMP2A [16,50–52]. Fumarylacetoacetate hydrolase (FAH) was used as a reference protein.

4.6. Measurement of energy-balance metabolites in liver tissue (gas chromatography)

Metabolomic analysis was performed as previously reported [53]. Briefly, 100 mg of liver tissue was placed in 1 mL of methanol/water (8:2), mixed with D4-succinic acid (MeOH-D4s) as a standard at a final concentration of 0.01 μM, and homogenized with a Precellys 24 homogenizer (Izasa, Barcelona, Spain). Samples were stored at −20 °C for 2 h to precipitate the proteins and centrifuged at 15,000 rpm for 10 min at 4 °C. The supernatants were collected and stored at −80 °C. At the moment of analysis, samples were dried with N_2 and derivatized with methoxylamine hydrochloride dissolved in pyridine (40 mg/mL) and *N*-methyl-*N*-trimethylsilyl trifluoroacetamide. Analyses were performed with a 7890A gas chromatograph coupled with an electron impact source to a 7200 quadrupole time-of-flight mass spectrometer (GC-MS-EI) (Agilent Technologies, Santa Clara, USA).

4.7. Measurement of glutathione, glutathione disulfide and methionine cycle-related metabolites (liquid chromatography)

Metabolites were measured as described [54]. For the most common methionine cycle-related metabolites, 25 mg of liver tissue was added to 1 mL of an extraction solution containing methanol:water (8:2 v/v), 1% ascorbic acid (m/v) and 0.5% β-mercaptoethanol (v/v) and homogenized with Precellys 24 homogenizer (Izasa). After protein precipitation, samples were centrifuged at 14,000 rpm for 10 min at 4 °C, the supernatant was collected, dried under N_2, resuspended in 100 μL of ultrapure type 1 water containing 50 mM ammonium acetate + 0.2% formic acid and placed into vials for analysis. Five milliliters of sample was injected into an ultrahigh-pressure liquid chromatography-quadrupole time of flight mass spectrometer (Agilent Technologies, Santa Clara, USA) (UHPLC). To attain optimal results, GSH and GSSG were measured individually. Briefly, 50 mg of liver tissue was added to 500 μL of 100 mM N-ethylmaleimide, 152 mM NaCl in 1 mM acetic acid, and homogenized with a Precellys 24 homogenizer (Izasa). We used 200 μL of 8 M trichloroacetic acid for cell lysis and protein precipitation. Then, N-ethylmaleimide was removed by adding 10 mL of dichloromethane. Samples were centrifuged at 14,000 rpm, 4 °C for 10 min, and 10 μL were injected into the UHPLC. Data quantification was performed using the calibration curves of each standard.

4.8. Statistical analyses

We used the nonparametric Mann-Whitney *U* tests for comparisons between two groups according to the distribution of results in the measured variables. For comparing more than two groups, the Kruskal-Wallis was used. All statistical analyses and relevant graphics were performed with GraphPad Prism software 6.01 (GraphPad Software, San Diego, CA, USA), SPSS Software (IBM SPSS Statistics for Windows, Version 21.00 Armonk, NY: IBM Corp) and MetaboAnalyst 3.0 (www.metaboanalyst.ca). Differences were considered statistically significant when the *P* value was ≤ 0.05. Unless otherwise indicated, the results are expressed as the mean ± standard error of the mean.

Declarations of interest

The authors declare no commercial or financial conflicts of interest.

Author contributions

FLM, JAM, JC, and JJ contributed to conception and design of the experimental plan. FLM, NC, GBG, SFA, AHA, ERT, MMG and JAM made substantial contributions to acquisition, analysis and interpretation of data. FLM, JC, and JJ participate in drafting the manuscript. All authors participate in revising the manuscript critically for important intellectual content. The guarantors for the overall content are Jordi Camps and Jorge Joven.

Transparency document

The Transparency document associated with this article can be found, in online version.

Acknowledgment

The authors thank Dr. Diana Shih, from the Division of Cardiology of the University of California in Los Angeles, for the generous gift of a breeding pair of PON1-deficient mice. This study was funded by grant PI15/00285 from the *Instituto de Salud Carlos III* (Madrid, Spain), co-funded by the *Fondo Europeo de Desarrollo Regional* (FEDER), and by grant 60/U/2016 from the *Fundació La Marató de TV3* (Barcelona, Spain). We also acknowledge the support provided by the *Agència de Gestió d'Ajuts Universitaris i de Recerca* (Grant 2016FI_B 00352) and the *Universitat Rovira i Virgili* (Grant URVPFRB21545). The funders had no role in study design, data collection and analysis, decision to publish, or preparation of the manuscript.

Appendix A. Supplementary data

Supplementary data to this article can be found online at https://doi.org/10.1016/j.bbadis.2019.03.006.

References

[1] G. Musso, M. Cassader, R. Gambino, Non-alcoholic steatohepatitis: emerging molecular targets and therapeutic strategies, Nat. Rev. Drug Discov. 15 (2016) 249–274, https://doi.org/10.1038/nrd.2015.3.

[2] V.T. Samuel, G.I. Shulman, Nonalcoholic fatty liver disease as a nexus of metabolic and hepatic diseases, Cell Metab. 27 (2018) 22–41, https://doi.org/10.1016/j.cmet.2017.08.002.

[3] M.C. Garcia, M. Amankwa-Sakyi, T.J. Flynn, Cellular glutathione in fatty liver in vitro models, Toxicol. in Vitro 25 (2011) 1501–1506, https://doi.org/10.1016/j.tiv.2011.05.011.

[4] C. Koliaki, J. Szendroedi, K. Kaul, T. Jelenik, P. Nowotny, F. Jankowiak, et al., Adaptation of hepatic mitochondrial function in humans with non-alcoholic fatty liver is lost in steatohepatitis, Cell Metab. 21 (2015) 739–746, https://doi.org/10.1016/j.cmet.2015.04.004.

[5] H.K. Vincent, A.G. Taylor, Biomarkers and potential mechanisms of obesity-induced oxidant stress in humans, Int. J. Obes. 30 (2006) 400–418, https://doi.org/10.1038/sj.ijo.0803177.

[6] R. Veteläinen, A. van Vliet, T.M. van Gulik, Essential pathogenic and metabolic differences in steatosis induced by choline or methione-choline deficient diets in a rat model, J. Gastroenterol. Hepatol. 22 (2007) 1526–1533, https://doi.org/10.1111/j.1440-1746.2006.04701.x.

[7] J. Camps, E. Rodríguez-Gallego, A. García-Heredia, I. Triguero, M. Riera-Borrull, A. Hernández-Aguilera, et al., Paraoxonases and chemokine (C-C motif) ligand-2 in noncommunicable diseases, Adv. Clin. Chem. 63 (2014), https://doi.org/10.1016/B978-0-12-800094-6.00007-8.

[8] A. García-Heredia, E. Kensicki, R.P. Mohney, A. Rull, I. Triguero, J. Marsillach, et al., Paraoxonase-1 deficiency is associated with severe liver steatosis in mice fed a high-fat high-cholesterol diet: a metabolomic approach, J. Proteome Res. 12 (2013) 1946–1955, https://doi.org/10.1021/pr400050u.

[9] A. Rull, F. Rodríguez, G. Aragonès, J. Marsillach, R. Beltrán, C. Alonso-Villaverde, et al., Hepatic monocyte chemoattractant protein-1 is upregulated by dietary cholesterol and contributes to liver steatosis, Cytokine 48 (2009) 273–279, https://doi.org/10.1016/j.cyto.2009.08.006.

[10] E. Rodríguez-Gallego, M. Riera-Borrull, A. Hernández-Aguilera, R. Mariné-Casadó, A. Rull, R. Beltrán-Debón, et al., Ubiquitous transgenic overexpression of C-C chemokine ligand 2: a model to assess the combined effect of high energy intake and continuous low-grade inflammation, Mediat. Inflamm. (2013) 1–19, https://doi.org/10.1155/2013/953841.

[11] F. Heymann, F. Tacke, Immunology in the liver — from homeostasis to disease, Nat. Rev. Gastroenterol. Hepatol. 13 (2016) 88–110, https://doi.org/10.1038/nrgastro.2015.200.

[12] L.A.J. O'Neill, E.J. Pearce, Immunometabolism governs dendritic cell and macrophage function, J. Exp. Med. 213 (2016) 15–23, https://doi.org/10.1084/jem.20151570.

[13] L. Xu, H. Kitade, Y. Ni, T. Ota, Roles of chemokines and chemokine receptors in obesity-associated insulin resistance and nonalcoholic fatty liver disease, Biomolecules 5 (2015) 1563–1579, https://doi.org/10.3390/biom5031563.

[14] A. Hernández-Aguilera, A. Rull, E. Rodríguez-Gallego, M. Riera-Borrull, F. Luciano-Mateo, J. Camps, et al., Mitochondrial dysfunction: a basic mechanism in inflammation-related non-communicable diseases and therapeutic opportunities, Mediat. Inflamm. 2013 (2013) 135698, , https://doi.org/10.1155/2013/135698.

[15] O.A. Lozoya, I. Martinez-Reyes, T. Wang, D. Grenet, P. Bushel, J. Li, et al., Mitochondrial nicotinamide adenine dinucleotide reduced (NADH) oxidation links the tricarboxylic acid (TCA) cycle with methionine metabolism and nuclear DNA methylation, PLoS Biol. 16 (4) (2018) e2005707, , https://doi.org/10.1371/journal.pbio.2005707.

[16] G. Filomeni, D. De Zio, F. Cecconi, Oxidative stress and autophagy: the clash between damage and metabolic needs, Cell Death Differ. 22 (2015) 377–388, https://doi.org/10.1038/cdd.2014.150.

[17] D.J. Klionsky, D.J. Klionsky, K. Abdelmohsen, A. Abe, M.J. Abedin, H. Abeliovich, et al., Guidelines for the use and interpretation of assays for monitoring autophagy (3rd edition), Autophagy 12 (2016) 1–222, https://doi.org/10.1080/15548627.2015.1100356.

[18] J.L. Schneider, A.M. Cuervo, Liver autophagy: much more than just taking out the trash, Nat. Rev. Gastroenterol. Hepatol. 11 (2014) 187–200, https://doi.org/10.1038/nrgastro.2013.211.

[19] M. Tous, N. Ferré, A. Rull, J. Marsillach, B. Coll, C. Alonso-Villaverde, et al., Dietary cholesterol and differential monocyte chemoattractant protein-1 gene expression in aorta and liver of apo E-deficient mice, Biochem. Biophys. Res. Commun. 340 (4) (2006) 1078–1084, https://doi.org/10.1016/j.bbrc.2005.12.109.

[20] A. Hernández-Aguilera, S. Fernández-Arroyo, E. Cuyàs, F. Luciano-Mateo, N. Cabre, J. Camps, et al., Epigenetics and nutrition-related epidemics of metabolic diseases: current perspectives and challenges, Food Chem. Toxicol. 96 (2016) 191–204, https://doi.org/10.1016/j.fct.2016.08.006.

[21] J. Lee, Y. Kim, S. Friso, S.W. Choi, Epigenetics in non-alcoholic fatty liver disease, Mol. Asp. Med. 54 (2017) 78–88, https://doi.org/10.1016/j.mam.2016.11.008.

[22] M. Riera-Borrull, A. García-Heredia, S. Fernández-Arroyo, A. Hernández-Aguilera, N. Cabré, E. Cuyàs, et al., Metformin potentiates the benefits of dietary restraint: a metabolomic study, Int. J. Mol. Sci. 18 (11) (2017), https://doi.org/10.3390/ijms18112263.

[23] E. Cuyàs, S. Fernández-Arroyo, S. Verdura, R.Á. García, J. Stursa, L. Werner, et al., Metformin regulates global DNA methylation via mitochondrial one-carbon metabolism, Oncogene. 37 (7) (2018) 963–970, https://doi.org/10.1038/onc.2017.367.

[24] S. Satapati, B. Kucejova, J.A. Duarte, J.A. Fletcher, L. Reynolds, N.E. Sunny, et al., Mitochondrial metabolism mediates oxidative stress and inflammation in fatty liver, J. Clin. Invest. 126 (4) (2016) 1605, https://doi.org/10.1172/JCI86695.

[25] S.E. Schriner, N.J. Linford, G.M. Martin, P. Treuting, C.E. Ogburn, M. Emond, et al., Extension of murine life span by overexpression of catalase targeted to mitochondria, Science. 308 (5730) (2005) 1909–1911, https://doi.org/10.1126/science.1106653.

[26] G. Nguyen, S.Y. Park, C.T. Le, W.S. Park, D.H. Choi, E.H. Cho, Metformin ameliorates activation of hepatic stellate cells and hepatic fibrosis by succinate and GPR91 inhibition, Biochem. Biophys. Res. Commun. 495 (4) (2018) 2649–2656, https://doi.org/10.1016/j.bbrc.2017.12.143.

[27] J.M. Mato, S.C. Lu, Role of S-adenosyl-L-methionine in liver health and injury, Hepatology 45 (2007) 1306–1312, https://doi.org/10.1002/hep.21650.

[28] N. Li, J. Hua, Immune cells in liver regeneration, Oncotarget. 8 (2) (2017) 3628–3639, https://doi.org/10.18632/oncotarget.12275.

[29] S. Hui, J.M. Ghergurovich, R.J. Morscher, C. Jang, X. Teng, W. Lu, et al., Glucose feeds the TCA cycle via circulating lactate, Nature. 551 (7678) (2017) 115–118, https://doi.org/10.1038/nature24057.

[30] Y.H. Youm, K.Y. Nguyen, R.W. Grant, E.L. Goldberg, M. Bodogai, D. Kim, et al., The ketone metabolite β-hydroxybutyrate blocks NLRP3 inflammasome-mediated inflammatory disease, Nat. Med. 21 (3) (2015) 263–269, https://doi.org/10.1038/nm.3804.

[31] T. Honda, M. Ishigami, F. Luo, M. Lingyun, Y. Ishizu, T. Kuzuya, et al., Branched-chain amino acids alleviate hepatic steatosis and liver injury in choline-deficient high-fat diet induced NASH mice, Metabolism. 69 (2017) 177–187, https://doi.org/10.1016/j.metabol.2016.12.013.

[32] M.M. Mihaylova, R.J. Shaw, The AMPK signalling pathway coordinates cell growth, autophagy and metabolism, Nat. Cell Biol. 13 (9) (2011) 1016–1023, https://doi.org/10.1038/ncb2329.

[33] D. Shao, S. Oka, T. Liu, P. Zhai, T. Ago, S. Sciarretta, et al., A redox-dependent mechanism for regulation of AMPK activation by Thioredoxin1 during energy starvation, Cell Metab. 19 (2) (2014) 232–245, https://doi.org/10.1016/j.cmet.2013.12.013.

[34] K. Frudd, T. Burgoyne, J.R. Burgoyne, Oxidation of Atg3 and Atg7 mediates inhibition of autophagy, Nat. Commun. 9 (2018) 95, , https://doi.org/10.1038/s41467-017-02352-z.

[35] M.J. Czaja, Function of autophagy in nonalcoholic fatty liver disease, Dig. Dis. Sci. 61 (5) (2016) 1304–1313, https://doi.org/10.1007/s10620-015-4025-x.

[36] S. Yan, N. Huda, B. Khambu, X.M. Yin, Relevance of autophagy to fatty liver diseases and potential therapeutic applications, Amino Acids 49 (12) (2017) 1965–1979, https://doi.org/10.1007/s00726-017-2429-y.

[37] J.L. Schneider, Y. Suh, A.M. Cuervo, Deficient chaperone-mediated autophagy in liver leads to metabolic dysregulation, Cell Metab. 20 (3) (2014) 417–432, https://doi.org/10.1016/j.cmet.2014.06.009.

[38] S. Kaushik, A.M. Cuervo, Degradation of lipid droplet-associated proteins by chaperone-mediated autophagy facilitates lipolysis, Nat. Cell Biol. 17 (6) (2015) 759–70, https://doi.org/10.1038/ncb3166.

[39] S. Kaushik, A.M. Cuervo, The coming of age of chaperone-mediated autophagy, Nat. Rev. Mol. Cell Biol. 19 (6) (2018) 365–381, https://doi.org/10.1038/s41580-018-0001-6.

[40] J.A. Rodriguez-Navarro, S. Kaushik, H. Koga, C. Dall'Armi, G. Shui, M.R. Wenk, et al., Inhibitory effect of dietary lipids on chaperone-mediated autophagy, Proc. Natl. Acad. Sci. U. S. A. 109 (12) (2012) E705–E714, https://doi.org/10.1073/pnas.1113036109.

[41] D. Martini, C. Del Bo', M. Porrini, S. Ciappellano, P. Riso, Role of polyphenols and polyphenol-rich foods in the modulation of PON1 activity and expression, J. Nutr. Biochem. 48 (2017) 1–8, https://doi.org/10.1016/j.jnutbio.2017.06.002.

[42] R. Beltrán-Debón, C. Alonso-Villaverde, G. Aragonès, I. Rodríguez-Medina, A. Rull, V. Micol, et al., The aqueous extract of Hibiscus sabdariffa calices modulates the production of monocyte chemoattractant protein-1 in humans, Phytomedicine. 17 (3–4) (2010) 186–191, https://doi.org/10.1016/j.phymed.2009.08.006.

[43] O. Krenkel, T. Puengel, O. Govaere, A.T. Abdallah, J.C. Mossanen, M. Kohlhepp, et al., Therapeutic inhibition of inflammatory monocyte recruitment reduces steatohepatitis and liver fibrosis, Hepatology. 67 (4) (2018) 1270–1283, https://doi.org/10.1002/hep.29544.

[44] S.L. Friedman, B.A. Neuschwander-Tetri, M. Rinella, A.J. Sanyal, Mechanisms of NAFLD development and therapeutic strategies, Nat. Med. 24 (2018) 908–922, https://doi.org/10.1038/s41591-018-0104-9.

[45] J. Joven, A. Rull, N. Ferré, J.C. Escolà-Gil, J. Marsillach, B. Coll, et al., The results in rodent models of atherosclerosis are not interchangeable, Atherosclerosis 195 (2007) e85–e92, https://doi.org/10.1016/j.atherosclerosis.2007.06.012.

[46] F. Rodríguez-Sanabria, A. Rull, R. Beltrán-Debón, G. Aragonès, J. Camps, B. Mackness, et al., Tissue distribution and expression of paraoxonases and chemokines in mouse: the ubiquitous and joint localisation suggest a systemic and coordinated role, J. Mol. Histol. 41 (2010) 379–386, https://doi.org/10.1007/s10735-010-9299-x.

[47] W. Liang, A.L. Menke, A. Driessen, G.H. Koek, J.H. Lindeman, R. Stoop, et al., Establishment of a general NAFLD scoring system for rodent models and comparison to human liver pathology, PLoS One 9 (2014) e115922, , https://doi.org/10.1371/journal.pone.0115922.

[48] C.L. Scott, F. Zheng, P. De Baetselier, L. Martens, Y. Saeys, S. De Prijck, et al., Bone

marrow-derived monocytes give rise to self-renewing and fully differentiated Kupffer cells, Nat. Commun. 7 (2016) 10321, , https://doi.org/10.1038/ncomms10321.
[49] O. Krenkel, F. Tacke, Liver macrophages in tissue homeostasis and disease, Nat. Rev. Immunol. 17 (2017) 306–321, https://doi.org/10.1038/nri.2017.11.
[50] D.A. Fruman, H. Chiu, B.D. Hopkins, S. Bagrodia, L.C. Cantley, R.T. Abraham, The PI3K pathway in human disease, Cell 170 (2017) 605–635, https://doi.org/10.1016/j.cell.2017.07.029.
[51] P.D. Pezze, S. Ruf, A.G. Sonntag, M. Langelaar-Makkinje, P. Hall, A.M. Heberle, et al., A systems study reveals concurrent activation of AMPK and mTOR by amino acids, Nat. Commun. 7 (2016) 13254, , https://doi.org/10.1038/ncomms13254.
[52] R. Pérez-Carro, R. Sánchez-Alcudia, B. Pérez, R. Navarrete, C. Pérez-Cerdá, M. Ugarte, et al., Functional analysis and *in vitro* correction of splicing *FAH* mutations causing tyrosinemia type I, Clin. Genet. 86 (2014) 167–171, https://doi.org/10.1111/cge.12243.
[53] M. Riera-Borrull, E. Rodríguez-Gallego, A. Hernández-Aguilera, F. Luciano, R. Ras, E. Cuyàs, et al., Exploring the process of energy generation in pathophysiology by targeted metabolomics: performance of a simple and quantitative method, J. Am. Soc. Mass Spectrom. 27 (2016) 168–177, https://doi.org/10.1007/s13361-015-1262-3.
[54] Å. Florholmen-Kjær, R.A. Lysså, O.-M. Fuskevåg, R. Goll, A. Revhaug, K.E. Mortensen, A sensitive method for the analysis of glutathione in porcine hepatocytes, Scand. J. Gastroenterol. 49 (2014) 1–8, https://doi.org/10.3109/00365521.2014.964757.